Originals

Computational Mechanics 18 (1996) 245–258 © Springer-Verlag 1996

Modelling and computation of instability phenomena in multisurface elasto-plasticity

E. Sawischlewski, P. Steinmann, E. Stein

Abstract This contribution is concerned with theoretical and numerical aspects of instability phenomena in multisurface elasto-plasticity which is the adequate constitutive framework for e.g. single crystal plasticity. To this end, the localization analysis for multisurface elasto-plasticity based on the additive decomposition of the geometrically linearized strain tensor is considered and the characteristic differences and similarities to the wellknown single surface case are highlighted. In the numerical part we subsequently discuss the computational setting of single crystal plasticity as the paradigm for multisurface elasto-plasticity. Finally, the numerical examples demonstrate the dramatic influence of the slip system orientation on the resulting localized failure mode of a single crystal compression panel.

1 Introduction

In *single surface* elasto-plasticity the stress state is limited by a yield condition which is expressed as a *single* scalar valued, *smooth* and convex tensor function of the stress tensor and generally a set of internal variables, consider as an example the classical v. Mises or Drucker-Prager criteria. By the way of contrast, *non smooth* yield criteria as for example the Tresca or Mohr-Coulomb models are characterized by several smooth yield surfaces intersecting in a non-smooth fashion at certain stress and internal variables states. Likewise, the formulation of *single crystal* plasticity involves a number of yield conditions associated with the possible slip systems within a crystal unit cell which might be activated simultaneously. (Watanabe and Atluri, 1986) elaborated on the unification of concepts of internal time, internal variables and multi yield surface theories to model nonlinear isotropic and kinematic hardening. (Rizzi, Maier and Willam 1996) refer to models of elasto-plasticity coupled to damage based on different loading functions as multi-dissipative materials. Recently, in order to provide a better prediction of shear band formation in metals (Ramakrishnan and Atluri, 1994) and Ramakrishnan, (Okada and Atluri, 1994) proposed a dual yield model consisting of a classical v. Mises yield surface and in addition a so called shear yield function which acts as a potential for a directional preferred part of the inelastic strain. Generally, all these different approaches allow for the *simultanous* activation of several constraints on the stress and the internal variables state, the so called yield surfaces, and may be recast in the framework of *multisurface* elasto-plasticity.

The objective of this contribution is on the one hand to provide a systematically treatise on the localization analysis within the setting of *multisurface* elasto-plasticity by deriving conditions for the onset of localization under the assumption of either *continuous* or *discontinuous* bifurcation of the strain rate field. Thereby, the possibility of *multiple* active constraints and its consequences within the localization analysis is of particular interest. On the other hand computational issues concerning the model problem of *single crystal* plasticity are considered as the numerical counterpart to the preceding analytical derivations.

Localization of inelastic deformations within narrow bands is a failure phenomenon which is frequently observed in laboratory experiments as well as in nature. Within standard continuum theory localization is considered as a spatial discontinuity of the velocity gradient (Rice, 1976) (Thomas, 1961). Analogous arguments in the context of planar acceleration waves in solids are found in the early work of (Hadamard, 1903) and in the contributions by (Hill, 1962) and (Mandel, 1962, 1966). Based on the assumption of a linear comparison solid in the sense of (Hill 1958), *continuous* bifurcation is thereby reflected by a singularity of the localization tensor. Nevertheless, so far the interesting case of *discontinuous* bifurcation has only been considered in the literature for the basic model of *single surface* elasto-plasticity, see e.g. the discussion in (Ottosen and Runesson, 1991).

For the sake of transparency we restrict ourselves in this study on *multisurface* elasto-plastic models at *small strains* which are based on the *additive* decomposition of the strain rate field together with the assumption of a free energy density which governs the *elastic* stress response.

Finally, as a model problem, we will be concerned with *single crystal* plasticity. Thereby, it is widely accepted, that models of *single crystal* plasticity may be considered as particular examples of *multisurface* plasticity, see for example the early contributions by (Koiter, 1960) and (Mandel, 1972). Therefore, the underlying motivation for the present investigation is mainly provided by the desire to treat and to understand instability problems arising in *single crystal* plasticity.

In this context, we will base the constitutive modelling on the traditional lines of the framework for anisotropic crystal slip plasticity set forth e.g. by (Hill, 1966), (Hill and Havner,

Communicated by S. N. Atluri, 26 March 1996

E. Sawischlewski, P. Steinmann, E. Stein
Institut für Baumechanik und Numerische Mechanik, Universität Hannover, D-30167 Hannover

Correspondence to: E. Stein

Dedicated to the 10 anniversary of Computational Mechanics

1982) and (Asaro, 1983) among others. As far as the algorithmic implementation is concerned we will resort to recent computational treatments of anisotropic single crystal plasticity which have been advocated e.g. by (Cuitiño and Ortiz, 1992), (Borja and Wren, 1993), (Miehe, 1996) and (Steinmann and Stein, 1996). Several numerical examples investigate the topic of localization problems in computational *single crystal* plasticity.

The paper is organized as follows:

- After introducing briefly the general setting of *multisurface* elasto-plasticity based on the additive decomposition of the geometrically linearized strain tensor we first investigate the conditions for *diffuse* failure which is characterized as the stationarity condition for the stress state. Thereby, the analysis relies on the simple structure of the corresponding elasto-plastic tangent operator in the form of a sum of rank 1 updates.
- Next, the general localization or rather admissibility condition for the maintainance of a spatial discontinuity of the velocity gradient field is established. Based on this result we then discuss the condition for the onset of *continuous* localization for the case of *multisurface* elasto-plasticity. Thereby, the simple structure of the tangent operator carries over the structure of the localization tensor and is thus frequently exploited. In particular, for multiple active constraints the determinant of the localization tensor is shown to be conveniently evaluated in terms of a new matrix containing the hardening moduli in a simple fashion. On the one hand, the critical hardening moduli, allowing for the onset of *continuous* localization, may be extracted from this matrix.
- On the other hand, it turns out in the subsequent investigation that the condition for the onset of *discontinuous* localization is determined by negative spectral properties of this matrix. The analysis reveals the important result that in contrast to the *single surface* case *discontinuous* localization may precede *continuous* localization if *multiple* constraints are active.
- For *triple*, *double* and *single surface* plasticity, equipped with a particular family of hardening moduli frequently employed in the cases of single crystal plasticity, examples of how to compute the critical hardening moduli are analysed in the sequel. Thereby, the intriguing results for either *latent* or pure *self hardening* of the slip systems are emphasized and the characteristic differences and similarities to the wellknown *single surface* case are highlighted.
- In the numerical part we first discuss the computational setting of *single crystal* plasticity as a paradigm for *multisurface* elasto-plasticity. Thereby, the restriction to a geometrically linearized format allows for a particular simple and transparent integration algorithm. Finally, in the numerical examples we focus on the dramatic influence of the slip system orientation on the resulting localized failure mode and load carrying capacity of a *single crystal* compression panel.

2 Multisurface plasticity

(Koiter, 1960) and (Mandel, 1972) considered models of *single crystal* plasticity as particular examples of *multisurface* plasticity. In *polycrystal* metal plasticity the classical Tresca yield condition or the recently proposed dual yield model by (Ramakrishnan and Atluri, 1994) may be considered as typical examples of *doublesurface* plasticity. (Watanabe and Atluri, 1986) demonstrated that models of nonlinear kinematic hardening may be recast within multi yield surface theories. Likewise, within soil mechanics the Mohr-Coulomb condition, the Cam-Clay and the cap models allow for the simultaneous activation of different loading functions and therefore fall into the framework of *multisurface* plasticity.

To set the stage for the subsequent developments, we briefly review some essential relations of geometrically linear *multisurface* elasto-plasticity. As usual, the underlying kinematical assumption is the *additive* decomposition of the total strain into an elastic and a plastic part

$$\varepsilon = \varepsilon_e + \varepsilon_p \quad \text{with} \quad \varepsilon = \nabla_x^{sym} u \quad \text{and} \quad u \in \mathbb{R}^{n_{dim}}. \tag{1}$$

For *multisurface* elasto-plasticity with n_{srf} isotropic hardening mechanisms, we restrict ourselves to only n_{srf} scalar internal variables κ_I to define the free energy density Ψ as

$$\Psi = \Psi^{mac}(\varepsilon_e) + \Psi^{mic}(\kappa_I) \quad \text{with} \quad \Psi^{mac}(\varepsilon_e) = \tfrac{1}{2}\varepsilon_e : \mathcal{E}_{el} : \varepsilon_e$$
$$\text{and} \quad I = 1 \ldots n_{srf}. \tag{2}$$

Here, $\mathcal{E}_{el}$ denotes the fourth order *elastic* tangent operator of the geometrically linear theory. From the Clausius-Duhem inequality and upon introducing the *additive* decomposition of the strain rate $\dot{\varepsilon}$ into an elastic and a plastic part, we obtain the *elastic* part of the constitutive law and the yield stresses Y_I, which are the dissipative stresses that are thermodynamically conjugated to κ_I, as

$$\sigma = \frac{\partial \Psi^{mac}}{\partial \varepsilon_e} = \mathcal{E}_{el} : \varepsilon_e \quad \text{and} \quad Y_I = \frac{\partial \Psi^{mic}}{\partial \kappa_I} \quad \forall I = 1 \ldots n_{srf}. \tag{3}$$

For *multisurface* elasto-plasticity the structure of the remaining dissipation inequality then suggests n_{srf} yield conditions Φ_I in terms of the stress measure σ and the yield stress Y_I

$$\Phi_I(\sigma, Y_I) = \varphi_I(\sigma) - Y_I \leqq 0 \quad \text{with} \quad \nu_I = \frac{\partial \varphi_I}{\partial \sigma} \quad \forall I = 1 \ldots n_{srf} \tag{4}$$

Here, the ν_I denote the normal to the yield conditions in the stress space. Moreover, for the general *non-associated* case a Koiter type flow rule in terms of the flow directions μ_I together with the evolution equations for the hardening variables κ_I are given by

$$\dot{\varepsilon}_p = \sum_{I=1}^{n_{srf}} \gamma_I \mu_I \quad \text{and} \quad \dot{\kappa}_I = \gamma_I \quad \forall I = 1 \ldots n_{srf}. \tag{5}$$

Finally, the evolution of the stress and the yield stresses Y_I renders the *elastic* tangent operator and the *hardening moduli* H_{IJ} sampled into the matrix H for later use

$$\dot{\sigma} = \mathcal{E}_{el} : \dot{\varepsilon}_e \quad \text{with} \quad \mathcal{E}_{el} = \frac{\partial^2 \Psi^{mac}}{\partial \varepsilon_e \partial \varepsilon_e}$$
$$\dot{Y}_I = \sum_{J=1}^{n_{srf}} H_{IJ} \gamma_J \quad \text{with} \quad H_{IJ} = \frac{\partial^2 \Psi^{mic}}{\partial \kappa_I \partial \kappa_J}. \tag{6}$$

The special case of *associated* plasticity is obtained upon substituting $\boldsymbol{\mu}_I$ by $\boldsymbol{\nu}_I$ whereby the principle of maximum dissipation will be satisfied. *Plastic-loading* and *elastic-unloading* conditions together with the requirement of consistency are expressed for each yield condition as

$$\gamma_I \geqq 0 \quad \Phi_I(\boldsymbol{\sigma}, Y_I) \leqq 0 \quad \gamma_I \Phi_I(\boldsymbol{\sigma}, Y_I) = 0$$

$$\text{and} \quad \gamma_I \dot{\Phi}_I(\boldsymbol{\sigma}, Y_I) = 0. \tag{7}$$

For *associated* plasticity the loading-unloading conditions follow from the optimality conditions that are implied by the principle of maximum dissipation. In terms of an optimization problem with n_{srf} inequality constraints they represent the classical Kuhn-Tucker complementary conditions. For *non-associated* plasticity they are rather postulated by physical reasoning. Since generally not all n_{srf} yield conditions are simultanously active, we define in addition the set of active constraints $\mathscr{A}$ by

$$\mathscr{A} = \{I \in \{1 \ldots n_{srf}\} | \Phi_I = 0 \text{ and } \gamma_I > 0\} \quad \text{with} \quad n_{act} = \dim \mathscr{A}. \tag{8}$$

We are now in the position to evaluate the consistency conditions for the Φ_I in Eq. 7.4 as

$$\dot{\Phi}_I = \boldsymbol{\nu}_I : \mathcal{E}_{el} : \dot{\boldsymbol{\varepsilon}} - \sum_{J \in \mathscr{A}} h_{IJ} \gamma_J = 0 \quad \forall I \in \mathscr{A} \tag{9}$$

Thereby, the coefficients of the $\boldsymbol{h}$ and $\boldsymbol{\eta}$-matrices follow by incorporating the flow rule $\dot{\boldsymbol{\varepsilon}}_p$ as given in Eq. 5 into Eq. 9 to render

$$h_{IJ} = \eta_{IJ} + H_{IJ} \quad \text{and} \quad \eta_{IJ} = \boldsymbol{\nu}_I : \mathcal{E}_{el} : \boldsymbol{\mu}_J. \tag{10}$$

In the case of plastic loading the plastic multipliers γ_I follow from Eq. 9 with $\dot{\Phi}_I = 0$. Introducing the pseudo surface normals $\tilde{\boldsymbol{\nu}}_I$ as an abbreviation, we thus obtain

$$\gamma_I = \tilde{\boldsymbol{\nu}}_I : \mathcal{E}_{el} : \dot{\boldsymbol{\varepsilon}} > 0 \quad \text{with} \quad \tilde{\boldsymbol{\nu}}_I = \sum_{J \in \mathscr{A}} h^{IJ} \boldsymbol{\nu}_J \quad \forall I \in \mathscr{A} \tag{11}$$

As a result we obtain the *elasto-plastic* tangent operator in the remarkably simple format of a sum of rank one updates

$$\boxed{\mathcal{E}_{ep} = \mathcal{E}_{el} - \sum_{I \in \mathscr{A}} \mathcal{E}_{el} : \boldsymbol{\mu}_I \otimes \tilde{\boldsymbol{\nu}}_I : \mathcal{E}_{el}.} \tag{12}$$

3
Diffuse failure

Diffuse failure is characterized by a singularity of the *elasto-plastic* tangent operator or, equivalently, by the limit point condition for the stress state, thereby the corresponding (right) critical strain rate is denoted by $\dot{\boldsymbol{\varepsilon}}_{cr}$

$$\mathcal{E}_{ep} : \dot{\boldsymbol{\varepsilon}}_{cr} = 0. \tag{13}$$

By taking the structure of the *multisurface* tangent operator in Eq. 12 into account, the singularity requirement rewrites as

$$\dot{\boldsymbol{\varepsilon}}_{cr} = \sum_{I \in \mathscr{A}} [\tilde{\boldsymbol{\nu}}_I : \mathcal{E}_{el} : \dot{\boldsymbol{\varepsilon}}_{cr}] \boldsymbol{\mu}_I \tag{14}$$

and thus the critical strain rate is given by the weighted sum of the flow directions $\boldsymbol{\mu}_I$

$$\boxed{\dot{\boldsymbol{\varepsilon}}_{cr} = \sum_{I \in \mathscr{A}} \gamma_I^{cr} \boldsymbol{\mu}_I \quad \text{with} \quad \gamma_I^{cr} = \tilde{\boldsymbol{\nu}}_I : \mathcal{E}_{el} : \dot{\boldsymbol{\varepsilon}}_{cr} > 0} \tag{15}$$

Obviously, the critical strain rate does not contain elastic contributions and thus characterizes a state of perfect plasticity which allows for purely plastic strain rates. Introducing $\dot{\boldsymbol{\varepsilon}}_{cr}$ from Eq. 15 into the definition of γ_I^{cr} we obtain the condition

$$\gamma_I^{cr} \doteq \sum_{J \in \mathscr{A}} [\tilde{\boldsymbol{\nu}}_I : \mathcal{E}_{el} : \boldsymbol{\mu}_J] \gamma_J^{cr} \quad \text{where} \quad \dot{\boldsymbol{\varepsilon}}_{cr} = \sum_{J \in \mathscr{A}} \gamma_J^{cr} \boldsymbol{\mu}_J, \tag{16}$$

therefore we conclude that the *elasto-plastic* tangent operator obeys a singularity with multiplicity n_{act} for vanishing hardening moduli H_{IJ} since the above requirement renders

$$\tilde{\boldsymbol{\nu}}_I : \mathcal{E}_{el} : \boldsymbol{\mu}_J \doteq \delta_{IJ} \rightsquigarrow \boldsymbol{\nu}_I : \mathcal{E}_{el} : \boldsymbol{\mu}_J \doteq \boldsymbol{\nu}_I : \mathcal{E}_{el} : \boldsymbol{\mu}_J + H_{IJ} \tag{17}$$

In summary the *elasto-plastic* tangent operator is n_{act} rank deficient as soon as all active constraints cease to harden simultaneously

$$\boxed{H_{IJ} = 0 \quad \forall I, J \in \mathscr{A} \rightsquigarrow \mathcal{E}_{ep} : \dot{\boldsymbol{\varepsilon}}_{cr} = 0 \quad \text{with} \quad \dot{\boldsymbol{\varepsilon}}_{cr} = \sum_{I \in \mathscr{A}} \gamma_I^{cr} \boldsymbol{\mu}_I} \tag{18}$$

Thereby, the flow directions $\boldsymbol{\mu}_I$ span the n_{act} dimensional space of critical strain rates. Typically, this situation might be encountered in the case of *isotropic* hardening where all hardening moduli H_{IJ} coincide, say with the modulus H. This particular hardening behaviour will frequenctly be addressed in the sequel.

4
Localized failure

Within classical continuum mechanics the kinematical structure of a possible jump $[\![\nabla_x \dot{\boldsymbol{u}}]\!]$ of the velocity gradient $\nabla_x \dot{\boldsymbol{u}}$ across a discontinuity surface Γ characterized by the surface normal $\boldsymbol{n}$ as depicted in Fig. 1 is given as

$$[\![\nabla_x \cdot \dot{\boldsymbol{u}}]\!] = \zeta \boldsymbol{m} \otimes \boldsymbol{n} \rightsquigarrow [\![\dot{\boldsymbol{\varepsilon}}]\!] = \zeta [\boldsymbol{m} \otimes \boldsymbol{n}]^{sym} \tag{19}$$

with amplitude ζ and jump vector $\boldsymbol{m}$. Thereby, the key requirement for the possible development of a discontinuity is the spatial continuity of the traction rate vector across the discontinuity, see e.g. Rice [1976], which may be expressed as

$$[\![\dot{\boldsymbol{t}}]\!] = \dot{\boldsymbol{t}}_+ - \dot{\boldsymbol{t}}_- = 0 \tag{20}$$

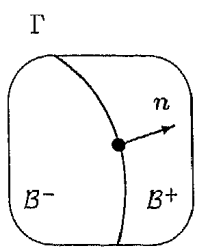

Fig. 1. Discontinuity Surface

Next, we use the definition of the traction rate $\dot{t} = \dot{\sigma} \cdot n$ to compute $\dot{t}_+$ and $\dot{t}_-$ on both sides of the discontinuity

$$\dot{t}_- = [\mathcal{E}_{ep}^- : \dot{\varepsilon}_-] \cdot n \quad \text{and} \quad \dot{t}_+ = [\mathcal{E}_{ep}^+ : \dot{\varepsilon}_+] \cdot n \tag{21}$$

and insert $\dot{\varepsilon}_+ = \dot{\varepsilon}_- + \zeta [m \otimes n]^{sym}$ to evaluate

$$\dot{t}_+ = \dot{t}_- + [[\![\mathcal{E}_{ep}]\!] : \dot{\varepsilon}_-] \cdot n + \zeta q_{ep} \cdot m. \tag{22}$$

Here, we introduced the *localization tensor* q_{ep} as the contraction of the tangent operator $\mathcal{E}_{ep}^+$ with the surface unit normal n to obtain

$$\boxed{q_{ep} = n \cdot \mathcal{E}_{ep}^+ \cdot n} \tag{23}$$

Thereby, the contractions are performed with respect to the second and fourth index of the fourth order tensor $\mathcal{E}_{ep}^+$. Moreover, we defined the jump in the tangent stiffness

$$[\![\mathcal{E}_{ep}]\!] = \mathcal{E}_{ep}^+ - \mathcal{E}_{ep}^- \tag{24}$$

since $\mathcal{E}_{ep}^+$ and $\mathcal{E}_{ep}^-$ might take, in general, different values in $\mathscr{B}^+$ and $\mathscr{B}^-$ due to the difference of ε_+ and ε_-.

From the traction continuity in Eq. (20) we establish the *localization* condition, or rather the *admissibility* condition for maintaining a discontinuity as

$$\boxed{[[\![\mathcal{E}_{ep}]\!]] : \dot{\varepsilon}_-] \cdot n + \zeta q_{ep} \cdot m = 0} \tag{25}$$

In the sequel we will examine the localization condition in Eq. 25 for different loading scenarios on both sides of the discontinuity under the assumption that no discontinuity has developed so far. Therefore, we concentrate on the investigation of the condition for the *onset* of localization. Thereby, we restrict ourselves to the basic case of *continuous* localization characterized by further plastic loading of all active constraints on both sides of the discontinuity and the limiting case of *discontinuous* localization where the domain $\mathscr{B}^-$ completely unloads elastically whereas the domain $\mathscr{B}^+$ continues to be loaded plastically for all active constraints.

5 Continuous localization

For multisurface *elasto-plasticity*, the situation of primary interest is characterized by continuous displacements across the *anticipated* discontinuity at the current state of deformation, i.e. no discontinuity has developed so far. For the onset of *continuous* localization we consider the case of *plastic loading* on both sides of the discontinuity, thus the jump in the *elasto-plastic* tangent operator vanishes identically

$$\mathcal{E}_{ep}^+ = \mathcal{E}_{ep}^- \rightsquigarrow [[\![\mathcal{E}_{ep}]\!]] = 0. \tag{26}$$

Upon introducing this result into Eq. 25, the condition for the *onset* of *continuous* localization is then formulated as

$$q_{ep} \cdot m = 0 \rightsquigarrow m \neq 0 \quad \text{if} \quad \det q_{ep} = 0. \tag{27}$$

Observe that the jump amplitude ζ does not come into play for this scenario. Taking into account the simple structure of $\mathcal{E}_{ep}$ in Eq. 12 results in an intriguing concise representation of the corresponding q_{ep} as a sum of rank 1 updates of the elastic localization tensor

$$\boxed{q_{ep} = q_{el} - \sum_{I \in \mathscr{A}} e_\mu^I \otimes \tilde{e}_\nu^I} \tag{28}$$

Here, the e_μ^I and $\tilde{e}_\nu^I$ may be interpreted as 'traction' vectors acting on the discontinuity surface and involve the flow directions μ_I and the pseudo yield surface normals $\tilde{\nu}_I$

$$e_\mu^I = [\mathcal{E}_{el} : \mu_I] \cdot n \quad \text{and} \quad \tilde{e}_\nu^I = [\tilde{\nu}_I : \mathcal{E}_{el}] \cdot n. \tag{29}$$

In the sequel it is our objective to evaluate the localization condition

$$\boxed{\det q_{ep} = 0} \tag{30}$$

for the case of *multisurface* plasticity in order to obtain explicit expressions for the critical hardening matrix H_{cr} which renders q_{ep} singular. Therefore, for the case of *multisurface* plasticity, we essentially have to compute the determinant of a n_{act} rank 1 update, thus extending the basic case of *singlesurface* plasticity discussed e.g. by (Ottosen and Runesson, 1991). Thereby, for the general case of *multisurface* plasticity, consider for example as a paradigm (fcc) or (bcc) single crystal plasticity, it appears convenient to introduce the *normalized elasto-plastic* localization tensor $\bar{q}_{el}$ as

$$\bar{q}_{ep} = q_{el}^{-1} \cdot q_{ep} \tag{31}$$

which represents a rank n_{act} update of the identity I by the 'projected' vectors $\bar{e}_\mu^I$ and the 'traction' vectors $\bar{e}_\nu^I$

$$\bar{q}_{ep} = I - \sum_{I \in \mathscr{A}} \bar{e}_\mu^I \otimes \tilde{e}_\nu^I \quad \text{with} \quad \bar{e}_\mu^I = q_{el}^{-1} \cdot e_\mu^I. \tag{32}$$

Next, we merely examine the eigenproblem for the update matrix, i.e. only the sum $\bar{e}_\mu^I \otimes \tilde{e}_\nu^I$ of rank 1 matrices. Here we follow lines advocated by (Rizzi, Maier and Willam, 1996) in the context of the geometrically linear theory for coupled models of plasticity and damage. To this end, we expand the right eigenvector into a sum $\alpha_J \bar{e}_\mu^J$ with unknown coefficients α_J. Thus, the $n_{dim} \times n_{dim}$ eigenproblem reads

$$\sum_{I,J \in \mathscr{A}} [\bar{e}_\mu^I \otimes \tilde{e}_\nu^I - \lambda_K I] \cdot [\alpha_J \bar{e}_\mu^J] = 0. \tag{33}$$

By inspection we readily extract the equivalent $n_{act} \times n_{act}$ eigenproblem for the $\tilde{\pi}$-matrix with coefficients $\tilde{\pi}_{IJ} = \tilde{e}_\nu^I \cdot \bar{e}_\mu^J$, maximum rank $\min(n_{dim}, n_{act})$ and the eigenvector α comprising the coefficients α_J as

$$\sum_{I,J \in \mathscr{A}} \bar{e}_\mu^I [\tilde{e}_\nu^I \cdot \bar{e}_\mu^J - \lambda_K \delta_{IJ}] \alpha_J = 0 \rightsquigarrow [\tilde{\pi} - \lambda_K I] \cdot \alpha = 0. \tag{34}$$

Please note that this result relies, however, on the linear independence of the 'projected' vectors $\bar{e}_\mu^I$. Clearly, for $n_{act} < n_{dim}$ the eigenvalues of the update matrix and the $\tilde{\pi}$-matrix are related via

$$\lambda_{1 \ldots n_{act}}(\tilde{\pi}) = \lambda_{1 \ldots n_{act}}\left(\sum_{I \in \mathscr{A}} \bar{e}_\mu^I \otimes \tilde{e}_\nu^I\right) \text{ and } \lambda_{> n_{act}}\left(\sum_{I \in \mathscr{A}} \bar{e}_\mu^I \otimes \tilde{e}_\nu^I\right) = 0. \tag{35}$$

Vice versa, for $n_{act} > n_{dim}$ the eigenvalues of the update matrix and the $\tilde{\pi}$ matrix are connected as

$$\lambda_{1\ldots n_{dim}}(\tilde{\pi}) = \lambda_{1\ldots n_{dim}}\left(\sum_{I\in\mathscr{A}} \bar{e}^I_\mu \otimes \tilde{e}^I_\nu\right) \text{ and } \lambda_{>n_{dim}}(\tilde{\pi}) = 0. \tag{36}$$

Moreover, the eigenvalues of the *normalized elasto-plastic* localization tensor $\bar{q}_{ep}$ and the update matrix $\sum_{I\in\mathscr{A}} \bar{e}^I_\mu \otimes \tilde{e}^I_\nu$ are connected by an eigenspectrum shift

$$\lambda_K(\bar{q}_{ep}) = 1 - \lambda_K\left(\sum_{I\in\mathscr{A}} \tilde{e}^I_\mu \otimes \tilde{e}^I_\nu\right) \quad \forall K = 1\ldots n_{dim} \tag{37}$$

whereas the eigenvectors $\alpha_J \bar{e}^J_\mu$ coincide. From these considerations we conclude straightforward that the determinant of $\bar{q}_{ep}$ is generally given by the *characteristic equation of* $\tilde{\pi}$ *at the eigenvalue* $\lambda(\tilde{\pi}) = 1$ or, equivalently, by the determinant of a newly introduced matrix $\omega = I - \tilde{\pi} \in \mathbb{R}^{n_{act}\times n_{act}}$. This intriguing result may be condensed in the following line of argumentation

$$\boxed{\begin{aligned}\det \bar{q}_{ep} &= \prod_{K=1}^{n_{dim}}\left[1 - \lambda_K\left(\sum_{I\in\mathscr{A}} \bar{e}^I_\mu \otimes \tilde{e}^I_\mu\right)\right] = \prod_{K=1}^{n_{act}}[1 - \lambda_K(\tilde{\pi})] \\ &= \det(I - \tilde{\pi}) = \det \omega\end{aligned}} \tag{38}$$

The matrix ω will play a prominent role in the subsequent derivations in the context of *discontinuous* localization. Based on this background we summarize our findings for the general *multisurface* case of the *elasto-plastic* localization tensor. Firstly, from Eq. (38) we obtain the determinant of q_{ep} with the generic structure

$$\boxed{\det q_{ep} = \det q_{el} \det \omega = \det q_{el}[1 - \tilde{\pi}:I + \cdots + [-1]^{n_{act}} \det \tilde{\pi}].} \tag{39}$$

Thereby the $\tilde{\pi}$ and π matrices with coefficients given by

$$\tilde{\pi}_{IJ} = \tilde{e}^I_\nu \cdot q_{el}^{-1} \cdot e^J_\mu \quad \text{and} \quad \pi_{IJ} = e^I_\nu \cdot q_{el}^{-1} \cdot e^J_\mu \quad \text{with} \quad \tilde{\pi} = h^{-1} \cdot \pi \tag{40}$$

together with the h and η matrices with coefficients given in Eq. (10) are $n_{act} \times n_{act}$ matrices. With $\det q_{el} > 0$ for properly formulated *elastic* constitutive models, the condition for the onset of *continuous* localization in Eq. (30) is recast, based on the *characteristic equation of* $\tilde{\pi}$ *at the eigenvalue* $\lambda(\tilde{\pi}) = 1$, into the simple expression

$$\boxed{\det \omega = \det(I - \tilde{\pi}) = 0} \tag{41}$$

By multiplying with $-\det h$ we obtain a formulation better suited for the actual computation of the critical hardening moduli contained in H_{cr}

$$\det(\pi - h) = \det(\bar{\eta} - H) = 0 \quad \text{where} \quad \bar{\eta} = \pi - \eta \tag{42}$$

thereby we invoked the $\bar{\eta}$ matrix $\in \mathbb{R}^{n_{act}\times n_{act}}$ with coefficients

$$\bar{\eta}_{IJ} = e^I_\nu \cdot q_{el}^{-1} \cdot e^J_\mu - \nu_I : \mathcal{E}_{el} : \mu_J. \tag{43}$$

Generally, the critical hardening moduli H_{cr}, rendering $\det q_{ep} = 0$, might be extracted from Eq. 42 in terms of the $\bar{\eta}$ matrix by invoking the explicit expression for the determinant of a sum of two $n_{act} \times n_{act}$ matrices. This line of arguments results in the structure

$$\boxed{\begin{aligned}&\det(\bar{\eta} - H) = \\ &\det \bar{\eta} + [-1]^{n_{act}} \det H - \operatorname{adj} \bar{\eta}:H + \cdots = 0 \quad \bar{\eta}, H \in \mathbb{R}^{n_{act}\times n_{act}}\end{aligned}} \tag{44}$$

The proof of this proposition follows immediately by e.g. assuming that $\bar{\eta}$ is nonsingular to render

$$\begin{aligned}\det(\bar{\eta} - H) &= \det \bar{\eta} \det(I - \bar{\eta}^{-1} \cdot H) \\ &= \det \bar{\eta}[\textit{characteristic equation of } \bar{\eta}^{-1} \\ &\quad \cdot H \textit{ at } \lambda(\bar{\eta}^{-1} \cdot H) = 1]\end{aligned} \tag{45}$$

Note that it is not necessary to compute explicitly the inverse $(\bullet)^{-1}$ of a matrix $(\bullet)$ in order to determine the coefficients of its *adjungate* matrix adj $(\bullet)$. In the analytical examples, which are postponed until the case of *discontinuous* localization is discussed, we will exploit Eq. 44 for a typical family of hardening moduli.

6 Discontinuous localization

Another possible loading situation within multisurface *elasto-plasticity* is characterized by *plastic loading* of all active constraints on the $\mathscr{B}^+$ side and complete *elastic unloading* on the $\mathscr{B}^-$ side of the *anticipated* discontinuity, while it is still assumed that no discontinuity has developed so far. The tangent operator on the $\mathscr{B}^+$ side of the discontinuity will then get an additional contribution due to the *plastic loading* condition in $\mathscr{B}^+$ such that

$$\mathcal{E}^+_{el} \neq \mathcal{E}^-_{ep} \quad \text{and} \quad [\![\mathcal{E}_{ep}]\!] = -\sum_{I\in\mathscr{A}} \mathcal{E}_{el} : \mu_I \otimes \tilde{\nu}_I : \mathcal{E}_{el}. \tag{46}$$

Upon introducing this result into Eq. 25 we obtain the condition for *onset* of *discontinuous* localization as

$$\boxed{\zeta q_{ep} \cdot m = \sum_{I\in\mathscr{A}} \gamma^-_I e^I_\mu.} \tag{47}$$

Here, γ^-_I denote the *negative* 'plastic multipliers', which reflect the *elastic unloading* condition on the $\mathscr{B}^-$ side of the discontinuity

$$\gamma^-_I = \tilde{\nu}_I : \mathcal{E}_{el} : \dot{\varepsilon}_- < 0. \tag{48}$$

Observe that the jump amplitude ζ is contained in the condition for *discontinuous* localization and, moreover, is indirectly driven by the strain rate $\dot{\varepsilon}_-$ on the $\mathscr{B}^-$ side of the discontinuity. Thereby, it turns out that the solution for the jump vector m is given by the sum of the 'projected' vectors $\bar{e}^I_\mu$ weighted

by factors $\tilde{\gamma}_J$ which in turn are related to the *negative* 'plastic multipliers' γ_I^-

$$\boxed{\zeta m = \sum_{J\in\mathscr{A}} \tilde{\gamma}_J \bar{e}_\mu^J \quad \text{with} \quad \tilde{\gamma}_J = \sum_{K\in\mathscr{A}} \omega^{JK}\gamma_K^- \quad \text{and} \quad \bar{e}_\mu^J = q_{el}^{-1}\cdot e_\mu^J} \tag{49}$$

Recall from the last section that the entries of the ω matrix are given by

$$\omega_{IJ} = \delta_{IJ} - \tilde{\pi}_{IJ} \quad \text{and} \quad \sum_{J\in\mathscr{A}} \omega_{IJ}\,\omega^{JK} = \delta_{IK}. \tag{50}$$

For a prove of this result insert the solution for the jump vector m into the lefthand side of Eq. (47) and consider the structure of the localization tensor in Eq. (28) to obtain

$$\zeta q_{ep}\cdot m = \zeta q_{el}\cdot m - \zeta \sum_{I\in\mathscr{A}} [\tilde{e}_\nu^I\cdot m]\, e_\mu^I = \sum_{I,J\in\mathscr{A}} [\delta_{IJ} - \tilde{\pi}_{IJ}]\tilde{\gamma}_J e_\mu^I$$

$$= \sum_{I\in\mathscr{A}} \gamma_I^-\, e_\mu^I \tag{51}$$

Finally we have to check under which condition the above localization mode complies with the assumed loading scenario. To this end, the strain rate $\dot{\varepsilon}_+ = \dot{\varepsilon}_- + \zeta[m\otimes n]^{sym}$ is incorporated into the definition of the γ_I^+ on the $\mathscr{B}^+$ side of the discontinuity

$$\gamma_I^+ = \tilde{\nu}_I : \varepsilon_{el} : \dot{\varepsilon}_+ = \tilde{\nu}_I : \mathcal{E}_{el} : \dot{\varepsilon}_- + \zeta\tilde{\nu}_I : \mathcal{E}_{el} : [m\otimes n] = \gamma_I^- + \zeta\tilde{e}_\nu^I\cdot m > 0. \tag{52}$$

Considering the localization mode as given in Eq. 49 results in the following line of argumentation

$$\gamma_I^+ = \gamma_I^- + \sum_{J\in\mathscr{A}} \tilde{\pi}_{IJ}\tilde{\gamma}_J = \sum_{I,K\in\mathscr{A}} [\omega_{IJ} + \tilde{\pi}_{IJ}]\omega^{JK}\gamma_K^- = \sum_{K\in\mathscr{A}} \omega^{JK}\gamma_K^- > 0. \tag{53}$$

Thus the positive multipliers γ_I^+ on the $\mathscr{B}^+$ side and the negative multipliers γ_I^- on the $\mathscr{B}^-$ side of the discontinuity are simply connected via the inverse of the ω matrix, and moreover we conclude that $\gamma_I^+ = \tilde{\gamma}_I$. Equivalently, the 'plastic multipliers' $\gamma_I^- < 0$ in $\mathscr{B}^-$ follow as

$$\gamma_I^- = \sum_{J\in\mathscr{A}} \omega_{IJ}\gamma_J^+ < 0. \tag{54}$$

Finally, the quadratic form of ω computed with vectors containing the γ_I^+ renders a strictly negative value

$$\sum_{I\in\mathscr{A}} \gamma_I^+\gamma_I^- = \sum_{I,J\in\mathscr{A}} \gamma_I^+\omega_{IJ}\gamma_J^+ = \frac{1}{2}\sum_{I,J\in\mathscr{A}} \gamma_I^+[\omega_{IJ} + \omega_{JI}]\gamma_J^+ < 0. \tag{55}$$

Thus, as a *necessary* condition, at least one eigenvalue of the symmetrized ω matrix ω^{sym} has to be negative in order to allow for *discontinuous* localization. Moreover, as a *sufficient* condition, all entries γ_I^+ in the corresponding eigenvector have to be strictly positive and have to be mapped into strictly negative values by the original matrix ω. A wellknown result in algebra, sometimes refered to as the Bromwich theorem, states that the eigenspectrum of a symmetrized matrix bounds the corresponding real eigenspectrum of the nonsymmetric matrix. Since $\omega = I - h^{-1}\cdot\pi$ is generally nonsymmetric, we therefore conclude that *discontinuous* localization may generally precede *continuous* localization which is characterized by a zero eigenvalue of the original ω matrix

$$\boxed{\lambda_{min}(\omega^{sym}) \leqq \Re(\lambda_{min}(\omega)).} \tag{56}$$

7
Analysis of continuous localization

In this section we will give examples of how to compute the critical hardening moduli for the *onset* of *continuous* localization in the case of *triple, double* and *single surface* plasticity. Thereby we resort to a common family of hardening moduli capable to describe *latent* as well as *self hardening*. We like to note that the following results coincide with the outcome of more direct but trite calculations based on the sequential application of the Sherman-Morrison formula and the corresponding formula for the determinant of a rank 1 update.

7.1
Critical hardening moduli for $n_{act} = 3$ and $n_{act} = 2$

On the one hand, the case of *triplesurface* plasticity is in a sense a limiting case in a three dimensional application $n_{dim} = 3$ since it leads to the maximum rank that might be obtained by the sum of linear independent dyadic products that updates the *elastic* localization tensor. On the other hand, typical examples for the case of *doublesurface* plasticity are the Asaro double slip kinematic within the framework of single crystal plasticity and likewise all plasticity models with two intersecting yield surfaces, e.g. certain cap models, where the two yield mechanisms might be activated simultaneously. Likewise, it was recently pointed out by (Rizzi, Maier and Willam, 1996) in the context of the geometrically linear theory that coupled models of plasticity and damage lead to a similar structure of the tangent operator. Moreover, the dual yield model proposed for metals by (Ramakrishnan and Atluri, 1994) fits neatly into the framework of *doublesurface* plasticity since it consists of the v. Mises yield surface and in addition a shear yield function which acts as a potential for the directional preferred part of the inelastic strain.

As generic expressions for these models, the *elasto-plastic* localization tensors for *triplesurface* and *doublesurface* plasticity with $n_{act} = 3$ or $n_{act} = 2$, respectively, are recast in the form of *three* or *two* rank 1 updates with the 'traction' vectors e_μ^I and $\tilde{e}_\nu^I$

$$q_{ep} = q_{el} - e_\mu^I \otimes \tilde{e}_\nu^1 - e_\mu^2 \otimes \tilde{e}_\nu^2 - e_\mu^3 \otimes \tilde{e}_\nu^3$$

$$\text{or} \quad q_{ep} = q_{el} - \tilde{e}_\mu^1 \otimes \tilde{e}_\mu^1 - e_\mu^2 \otimes \tilde{e}_\nu^2. \tag{57}$$

Based on the previous discussion, the determinant $\det \bar{q}_{ep}$ for the cases of *triplesurface* or *doublesurface* plasticity follows easily as

$$\boxed{\begin{aligned} &\det \bar{q}_{ep} = [1 - \tilde{\pi}:I + \operatorname{adj}\tilde{\pi}:I - \det\tilde{\pi}] \quad \text{or} \\ &\det \bar{q}_{ep} = [1 - \tilde{\pi}:I + \det\tilde{\pi}] \end{aligned}} \tag{58}$$

Recall that the terms in brackets might be interpreted as the *characteristic equations at the eigenvalue* $\lambda(\tilde{\pi}) = 1$ of matrices $\tilde{\pi}$. Thereby, in the *triplesurface* case, $\tilde{\pi}:I$, $\operatorname{adj}\tilde{\pi}:I$ and $\det\tilde{\pi}$ represent the three invariants of $\tilde{\pi}\in\mathbb{R}^{3\times3}$. Equivalently, for the *doublesurface* case, $\tilde{\pi}:I$ and $\det\tilde{\pi}$ denote the two invariants of $\tilde{\pi}\in\mathbb{R}^{2\times2}$.

To ease notation we will in the sequel tacitly understand that the proper dimension of the $\tilde{\pi}$, π, h, η, $\bar{\eta}$ and H matrices is either $n_{act} = 3$ or $n_{act} = 2$, respectively.

With this preliminaries at hand and with $\det q_{el} > 0$ for properly formulated *elastic* constitutive models, the localization condition in Eq. 58 may be rewritten according to Eq. 42 as $\det(\bar{\eta} - H) = 0$. It is interesting that we will encounter a similar structure for the basic *singlesurface* case in the sequel. For the *triplesurface* case the critical hardening moduli H_{cr}, rendering $\det q_{ep} = 0$, are then extracted from Eq. 42 in terms of the $\bar{\eta}$ matrix by invoking the explicit expression for the determinant of a sum of two matrices $\in\mathbb{R}^{3\times3}$, see e.g. de Boer [2]

$$\boxed{\begin{aligned}&\det(\bar{\eta} - H) = \det\bar{\eta} - \det H + \bar{\eta}:\operatorname{adj}H - \operatorname{adj}\bar{\eta}:H = 0\\ &\text{for}\quad \bar{\eta}, H\in\mathbb{R}^{3\times3}\end{aligned}} \tag{59}$$

Equivalently, in the *doublesurface* case the critical hardening moduli H_{cr} are extracted from Eq. 42 in terms of the $\bar{\eta}$ matrix by invoking the explicit expression for the determinant of a sum of two matrices $\in\mathbb{R}^{2\times2}$ as

$$\boxed{\det(\bar{\eta} - H) = \det\bar{\eta} + \det H - \operatorname{adj}\bar{\eta}:H = 0 \quad \text{for} \quad \bar{\eta}, H\in\mathbb{R}^{2\times2}.} \tag{60}$$

Here, $\operatorname{adj}\bar{\eta} = \det\bar{\eta}\,\bar{\eta}^{-t}$ and $\operatorname{adj}H = \det H\,H^{-t}$ and denote the *adjungate* matrices of $\bar{\eta}$ and H.

Explicit expressions for the critical moduli H_{cr} are derived in the following for the one parameter family of hardening moduli H proposed by (Hutchinson, 1970) in the context of single crystal plasticity. These hardening moduli are particularized for $n_{act} = 3$ and $n_{act} = 2$ as

$$H = H[\ell i + [1 - \ell]I]$$

$$\text{with either}\quad i = \begin{bmatrix}1&1&1\\1&1&1\\1&1&1\end{bmatrix}\quad\text{or}\quad i = \begin{bmatrix}1&1\\1&1\end{bmatrix}. \tag{61}$$

Here, the parameter H is a scalar valued reference hardening modulus. For single crystals the latent hardening parameter ℓ typically takes values $1 \leqq \ell \leqq 1.4$, see (Kocks, 1970). As a special case we first consider *latent hardening* of the slip systems for $\ell = 1$. Here, this type of *isotropic* Taylor hardening results in $\det H = 0$ and $\operatorname{adj}H = 0$. Then Eqs. 59 and 60 render

$$\det\bar{\eta} - H\operatorname{adj}\bar{\eta}:i = 0 \tag{62}$$

from which we explicitly compute the critical hardening modulus in terms of the sum of all coefficients of $\bar{\eta}^{-1}$

$$\boxed{H_{cr} = \max_{|n|=1}[\bar{\eta}^{-1}:i]^{-1}} \tag{63}$$

Next we examine the other limiting case of pure *self hardening* of the slip systems for $\ell = 0$. This particular Koiter hardening model leads to the simplifications $\det H = H^3$, $\operatorname{adj}H = H^2 I$ for $H\in\mathbb{R}^{3\times3}$ and $\det H = H^2$ for $H\in\mathbb{R}^{2\times2}$, respectively. Accordingly, Eqs. 59 and 60 transform into

$$-H^3 + H^2\bar{\eta}:I - H\operatorname{adj}\bar{\eta}:I + \det\bar{\eta} = 0$$

$$\text{or}\quad H^2 - H\operatorname{adj}\bar{\eta}:I + \det\bar{\eta} = 0 \tag{64}$$

which are the characteristic equations for $\bar{\eta}$ with $H = \lambda(\bar{\eta})$ corresponding to the eigenvalues of $\bar{\eta}$. Therefore, the critical hardening modulus is explicitly computed by the eigenvalue problem for $\bar{\eta}$

$$\boxed{H_{cr} = \max_{|n|=1}\max_{K}\lambda_K(\bar{\eta})} \tag{65}$$

In a general situation characterized e.g. by *overshooting* of the slip systems with $\ell > 1$, for which in fact experimental evidence was provided by Kocks [11], it is easily verified that the critical hardening modulus H_{cr} for the *triplesurface* and the *doublesurface* case follows from the roots of either a *cubic* or a *quadratic* polynomial in H, respectively.

As an extension of the previous results, we may summarize the analysis of the critical hardening moduli for the onset of *continuous* localization in the case of *multisurface* plasticity by the sequence of steps given in Table 1.

7.2 Critical hardening moduli for $n_{act} = 1$

In order to highlight the characteristic similarities between the cases with $n_{act} = 1$ and the cases of *multisurface* plasticity $n_{act} > 1$, we finally briefly reiterate the results obtained in the basic case of *singlesurface* plasticity as discussed in detail e.g. in (Ottosen and Runesson, 1991). Here, the *elasto-plastic* localization tensor boils down to only *one* rank 1 update and is given together with its determinant by the simple expression

$$q_{ep} = q_{el} - e_\mu\otimes\tilde{e}_\nu \quad\text{and}\quad \det q_{ep} = \det q_{el}[1 - \tilde{\pi}]. \tag{66}$$

Thereby, similar to the *multisurface* case, we introduce the $\tilde{\pi}$, π, h and η 'matrices' $\in\mathbb{R}$ as the products of the inverse of the *hyperelastic* localization tensor and the 'traction' vectors e_μ and $\tilde{e}_\nu$

$$\tilde{\pi} = \tilde{e}_\nu\cdot q_{el}^{-1}\cdot e_\mu,\quad \tilde{\pi} = h^{-1}\pi,\quad \pi = e_\nu\cdot q_{el}^{-1}\cdot e_\mu,$$

$$h = \eta + H \quad\text{with}\quad \eta = \nu:\mathcal{E}_{el}:\mu. \tag{67}$$

With this notation at hand and since $\det q_{el} > 0$ holds for properly formulated *elastic* constitutive models, the localization

Table 1. Analysis of *continuous* localization in *multisurface* plasticity

- Compute the η-matrix with entries $\eta_{IJ} = \nu_I:\mathcal{E}_{el}:\mu_J$
- Compute the π-matrix with entries $\pi_{IJ} = e_\nu^I\cdot q_{el}^{-1}\cdot e_\mu^J$
- Analyse $\bar{\eta} = \pi - \eta$ to obtain the critical hardening moduli H_{cr}
- Typical results: $H_{cr} = \max_{|n|=1}[\bar{\eta}^{-1}:i]^{-1}$ or $H_{cr} = \max_{|n|=1}\max_{K}\lambda_K(\bar{\eta})$

condition may be rewritten from Eq. 66.2 as

$$1-\tilde{\pi}=0 \rightsquigarrow \bar{\eta}-H=0 \quad \text{with} \quad \bar{\eta}=\pi-\eta=\boldsymbol{e}_\nu\cdot\boldsymbol{q}_{el}^{-1}\cdot\boldsymbol{e}_\mu-\boldsymbol{\nu}:\mathcal{E}_{el}:\boldsymbol{\mu}. \tag{68}$$

Finally, the critical hardening modulus H_{cr}, rendering $\det \boldsymbol{q}_{ep}=0$, is derived straightforward in terms of the $\bar{\eta}$ 'matrix' or equivalently in the more familiar expanded format

$$\boxed{H_{cr}=\max_{|n|=1}\bar{\eta}=\max_{|n|=1}(\boldsymbol{e}_\nu\cdot\boldsymbol{q}_{el}^{-1}\cdot\boldsymbol{e}_\mu)-\boldsymbol{\nu}:\mathcal{E}_{el}:\boldsymbol{\mu}.} \tag{69}$$

We conclude that no localization can occur as long as $H>H_{cr}$.

Moreover, the condition for *discontinuous localization* takes a particular intriguing format in the case of *singlesurface* plasticity since the $\boldsymbol{\omega}$ matrix boils down to a scalar $\omega<0$ thus rendering

$$\det \boldsymbol{q}_{ep}=\det \boldsymbol{q}_{el}\omega<0 \rightsquigarrow \gamma^+>0 \quad \text{and} \quad \gamma^-=\omega\gamma^+<0. \tag{70}$$

Thereby, ω happens to coincide with the smallest eigenvalue $\lambda_{min}(\bar{\boldsymbol{q}}_{ep})$ of the normalized localization tensor $\bar{\boldsymbol{q}}_{ep}$. Thus, *discontinuous* localization is possible as soon as the localization tensor obeys a negative eigenvalue.

8 Computational single crystal plasticity

8.1 Formulation of rate independent single crystal plasticity

As a paradigm of *associated* but *anisotropic* multisurface plasticity we consider the example of single crystal plasticity in the format advocated e.g. by (Asaro, 1983). Here, the flow rule is dictated by the kinematics of dislocation flow along fixed slip systems characterized by the slip direction $\boldsymbol{s}_I$ and the slip plane normal $\boldsymbol{m}_I$ in the so-called *isoclinic* configuration

$$\dot{\varepsilon}_p=\sum_{I\in\mathcal{A}}\gamma_I\boldsymbol{\nu}_I \quad \text{with} \quad \boldsymbol{\nu}_I=[\boldsymbol{s}_I\otimes\boldsymbol{m}_I]^{sym}. \tag{71}$$

Here the plastic multipliers γ_I take the interpretation as the slip rates on the slip systems I. Please note that plastic flow is assumed to preserve the plastic volume since we have simple shear with $\boldsymbol{s}_I\perp\boldsymbol{m}_I$ for each crystallographic slip system I. Typically, for fcc crystals we have 12 slip systems which might be activated in a general deformation. These are given by the four $\boldsymbol{m}_I\in\{111\}$ planes and the three $\boldsymbol{s}_I\in[110]$ directions of a crystal unit cell, see Fig. 2.

For the sake of simplicity we restrict ourselves to the geometrically linear case and assume the *elastic* response to be governed by the *isotropic* Hooke model valid for small strains

$$\mathcal{E}_{el}=2G\mathcal{I}^{dev}+K\boldsymbol{I}\otimes\boldsymbol{I} \quad \text{with} \quad \mathcal{I}^{dev}=\mathcal{I}-\tfrac{1}{3}\boldsymbol{I}\otimes\boldsymbol{I}. \tag{72}$$

Next, the so called Schmid tensor $\boldsymbol{\nu}_I$ projects the stress tensor $\boldsymbol{\sigma}$ or rather the deviatoric stress tensor $\boldsymbol{s}$ onto the shear stress $\tau_I\equiv\varphi_I$ which acts in the slip systems I, frequently refered to as the Schmid stress

$$\tau_I=\boldsymbol{s}:\boldsymbol{\nu}_I \quad \text{with} \quad \boldsymbol{s}=2G\boldsymbol{e}_e \quad \text{and} \quad \boldsymbol{e}_e=\mathcal{I}^{dev}:\boldsymbol{\varepsilon}_e. \tag{73}$$

Then the yield condition for each slip system is defined in terms of the Schmid stress and the critical shear flow stress, which will be denoted by $\tau_y^I\equiv Y_I$, as

$$\Phi_I=\tau_I-\tau_y^I\leqq 0 \tag{74}$$

To describe *isotropic* Taylor hardening of Al-Cu alloys, the *micro* part of the Helmholtz free energy Ψ^{mic} is typically expanded as

$$\Psi^{mic}(\kappa)=\tau_0\kappa+\frac{[\tau_\infty-\tau_0]^2}{H_0}\ln\left(\cosh\left(\frac{H_0\kappa}{\tau_\infty-\tau_0}\right)\right) \tag{75}$$

with τ_0 and τ_∞ the initial shear yield stress and the saturation strength, H_0 the initial hardening rate and the *isotropic* hardening variable κ defined as

$$\dot{\kappa}=\sum_{I\in\mathcal{A}}\gamma_I. \tag{76}$$

Then the critical shear flow stress $\tau_y=\tau_y^I$ and its derivative $H=\partial_\kappa\tau_y=H_{IJ}$ follow in closed form

$$\tau_y(\kappa)=\tau_0+[\tau_\infty-\tau_0]\tanh\left(\frac{H_0\kappa}{\tau_\infty-\tau_0}\right)$$

$$\text{and} \quad H(\kappa)=H_0\cosh^{-2}\left(\frac{H_0\kappa}{\tau_\infty-\tau_0}\right). \tag{77}$$

The constitutive model of small strain single crystal plasticity is summarized for convenience in Table 2.

8.2 Integration of rate independent single crystal plasticity

For the integration algorithm of the plastic strain rate in Eq. 71 it proves convenient to explicitly compute the $\boldsymbol{\eta}$ and the $\boldsymbol{h}$ matrices in terms of the slip direction $\boldsymbol{s}_I$ and the slip plane normal $\boldsymbol{m}_I$ as

$$\eta_{IJ}=2G\boldsymbol{\nu}_I:\boldsymbol{\nu}_J=G[[\boldsymbol{s}_I\cdot\boldsymbol{s}_J][\boldsymbol{m}_I\cdot\boldsymbol{m}_J]+[\boldsymbol{m}_I\cdot\boldsymbol{s}_J][\boldsymbol{s}_I\cdot\boldsymbol{m}_J]]$$

$$\text{and} \quad h_{IJ}=\eta_{IJ}+H \tag{78}$$

With this preliminaries at hand the deviatoric part of the plastic flow rule and the hardening variable are integrated over a finite

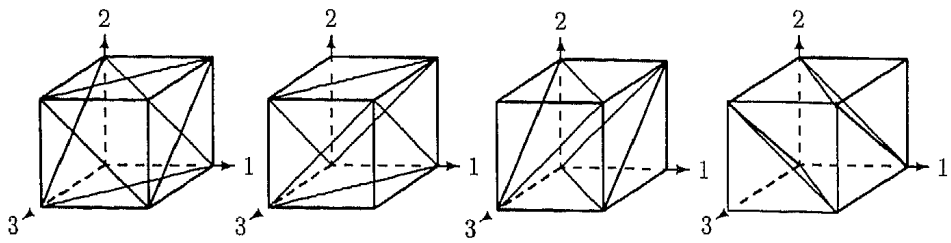

Fig. 2. Slip Systems of a fcc Crystal Unit Cell

Table 2. Constitutive equations of small strain single crystal plasticity

- *Macroscopic* and *Microscopic* Free Energy

$$\Psi^{mac} = G\, e_e : e_e + \frac{1}{2} K\, [I : \varepsilon]^2$$

$$\Psi^{mic} = \tau_0 \kappa + \frac{[\tau_\infty - \tau_0]^2}{H_0} \ln\left(\cosh\left(\frac{H_0 \kappa}{\tau_\infty - \tau_0}\right)\right)$$

- Yield Conditions

$$\Phi_I = \tau_I - \tau_y \leqq 0 \quad \text{with} \quad \tau_I = s : \nu_I \quad \text{and} \quad \nu_I = [s_I \otimes m_I]^{sym}$$

- Flow Rule and Evolution Law for the Hardening Variable

$$\dot{\varepsilon}_p = \sum_{I \in \mathscr{A}} \gamma_I\, \nu_I \quad \text{and} \quad \dot{\kappa} = \sum_{I \in \mathscr{A}} \gamma_I$$

- Elasto-Plastic Tangent Operator

$$\mathcal{E}_{ep} = \mathcal{E}_{el} - 4G^2 \sum_{I,J \in \mathscr{A}} h^{IJ}\, [s_I \otimes m_I]^{sym} \otimes [s_J \otimes m_J]^{sym}$$

time step $\Delta t = {}^{n+1}t - {}^{n}t$ by the Euler backward method to render

$$\Delta e_p = \sum_{I \in \mathscr{A}} \Delta\gamma_I\, \nu_I \quad \text{and} \quad \Delta\kappa = \sum_{I \in \mathscr{A}} \Delta\gamma_I \quad \text{with} \quad \Delta\gamma_I = \Delta t \gamma_I \tag{79}$$

Equivalently, we obtain the update for the deviatoric stresses with ${}^{e}s$ denoting the deviatoric *trial* stresses as

$${}^{n+1}s = {}^{e}s - 2G \sum_{I \in \mathscr{A}} \Delta\gamma_I\, \nu_I \quad \text{with} \quad {}^{e}s = 2G\,[{}^{n+1}e - {}^{n}e_p]. \tag{80}$$

Moreover, the updated Schmid stresses follow in terms of the *trial* Schmid stresses and the incremental slip rates as

$${}^{n+1}\tau_I = {}^{e}\tau_I - \sum_{J \in \mathscr{A}} \Delta\gamma_J\, \eta_{IJ}. \tag{81}$$

Finally, the unknwon incremental slip rates $\Delta\gamma_I$ are then determined from the solution of the implicit algorithmic consistency condition

$${}^{n+1}\Phi_I = {}^{n+1}\tau_I - \tau_y({}^{n}\kappa + \Delta\kappa) \doteq 0. \tag{82}$$

Thereby, one step of the local Newton iteration for the $\Delta\gamma_I$ is given in combination with a projection onto $\Delta\gamma_I \in \mathbb{R}_+$ as

$$\partial_{\Delta\gamma_J}\, {}^{n+1}\Phi_I = -\eta_{IJ} - H = -h_{IJ}$$

$$\rightsquigarrow \Delta\gamma_I = \max\left\{\left(\Delta\gamma_I + \sum_{J \in \mathscr{A}} h^{IJ}\, \Phi_J\right), 0\right\}. \tag{83}$$

In computational single crystal plasticity we typically encounter two major difficulties. Firstly, the choice of the active slip systems is ambiguous and thus not trivial. Therefore, we resort to an algorithm advocated by (Cuitiño and Ortiz, 1992) which includes the most loaded slip system into the active set after the local Newton iteration, based on the old active set, has converged. This outer loop is repeated until all yield conditions are satisfied. The problem of controlling the active slip systems has recently attracted much interest. Alternatively, thermodynamical considerations suggest to base the choice of the active slip systems on the local dissipation power.

Secondly, the active slip systems might not be linearly independent, thus prohibiting the inversion of the h_{IJ} matrix necessary for the local Newton iteration. Here we apply a back substitution filter technique proposed by (Borja and Wren, 1993) to suppress the linear dependent equations. Typically, this problem is not encountered in classical algorithmic treatments of *multi-surface* elasto-plasticity with linearly independent constraints as discussed in detail in (Simo, Kennedy and Govindjee, 1988). The integration algorithm is summarized for convenience in Table 3.

Finally, by linearizing the stress update formula in Eq. 80 and exploiting $\mathrm{d}\Phi_I \doteq 0$ for all slip systems $I \in \mathscr{A}$ we obtain

$$\mathrm{d}s = 2G\, \mathrm{d}e - 2G \sum_{I \in \mathscr{A}} \mathrm{d}\gamma_I\, \nu_I$$

$$\text{with} \quad \mathrm{d}\Phi_I = 2G\, \nu_I : \mathrm{d}e - \sum_{J \in \mathscr{A}} h_{IJ}\, \mathrm{d}\gamma_J = 0 \tag{84}$$

and thus the algorithmic tangent operator, necessary for the optimal convergence of the global Newton-Raphson equilib-

Table 3. Integration Algorithm for Small Strain Single Crystal Plasticity

1. Increment Initialization $\eta_{IJ} = 2G\, \nu_I : \nu_J$, $\mathscr{A} = \varnothing$ and *Trial* State

   ${}^{e}s = 2G[{}^{n+1}e - {}^{n}e_p]$ ${}^{e}\tau_I = {}^{e}s : \nu_I$ ${}^{e}\kappa = {}^{n}\kappa$ ${}^{e}\Phi_I = {}^{e}\tau_I - \tau_y({}^{e}\kappa)$

2. Iteration Initialization ${}^{n+1}\Phi_I = {}^{e}\Phi_I$, ${}^{n+1}\kappa = {}^{e}\kappa$ and $\Delta\gamma_I = 0$

3. Newton Step with Iteration Matrix $h_{IJ} = \eta_{IJ} + H({}^{n+1}\kappa)$, Projection and Filter

   $$\Delta\gamma_I = \max\left\{\left(\Delta\gamma_I + \sum_{J \in \mathscr{A}} h^{IJ}\, {}^{n+1}\Phi_J\right), 0\right\} \quad \mathscr{A} = \mathscr{A} / I\,(\Delta\gamma_I = 0)$$

4. Iteration Update

   ${}^{n+1}\tau_I = {}^{e}\tau_I - \sum_{J \in \mathscr{A}} \Delta\gamma_J\, \eta_{IJ}$ ${}^{n+1}\kappa = {}^{e}\kappa + \sum_{I \in \mathscr{A}} \Delta\gamma_I$ ${}^{n+1}\Phi_I = {}^{n+1}\tau_I - \tau_y({}^{n+1}\kappa)$

5. Check Residuum for Active Slip Systems

   If $\sum_{I \in \mathscr{A}} |{}^{n+1}\Phi_I|^2 \geqq \mathrm{Tol}^2$ then Goto 3

6. Check Residum for All Slip Systems

   with ${}^{n+1}\Phi_I^+ = \max\{{}^{n+1}\Phi_I, 0\}$

   If $\sum_{I=1}^{n_{inf}} |{}^{n+1}\Phi_I^+|^2 \geqq \mathrm{Tol}^2$ then $\mathscr{A} = \mathscr{A} \cup I\,(\max {}^{n+1}\Phi_I^+)$ and Goto 2

7. Increment Update

   ${}^{n+1}s = {}^{e}s - 2G \sum_{I \in \mathscr{A}} \Delta\gamma_I\, \nu_I$, ${}^{n+1}\kappa = {}^{e}\kappa + \sum_{I \in \mathscr{A}} \Delta\gamma_I$

8. Algorithmic Elasto-Plastic Tangent Operator

   $$\mathcal{E}^a_{ep} = \mathcal{E}_{el} - 4G^2 \sum_{I,J \in \mathscr{A}} h^{IJ}\, [s_I \otimes m_I]^{sym} \otimes [s_J \otimes m_J]^{sym}$$

rium iteration, is given by

$$d\sigma = \mathcal{E}^a_{ep} : d\varepsilon \quad \text{with} \quad \mathcal{E}^a_{ep} = \mathcal{E}_{el} - 4G^2 \sum_{I,J \in \mathcal{A}} h^{IJ} \nu_I \otimes \nu_J. \tag{85}$$

Please recall from the discussion in the previous section on diffuse failure that $\mathcal{E}^a_{ep}$ is singularized as soon as the slip systems cease to harden isotropically with $H = 0$. Thereby, the active flow directions ν_I span the space of critical strain increments $d\varepsilon_{cr}$. Moreover it is remarkable, that the algorithmic tangent operator $\mathcal{E}^a_{ep}$ coincides with the differential format of the tangent operator $\mathcal{E}_{ep}$ which is due to the linearity of the yield conditions of σ. Usually for common plasticity models as e.g. the v. Mises model the operators $\mathcal{E}_{ep}$ and $\mathcal{E}^a_{ep}$ differ due to finite load steps.

8.3
Extension to rate dependent single crystal plasticity

It is common in single crystal plasticity to allow for rate dependent behaviour by stating explicitly a viscoplastic evolution law for the slip rates γ_I on the slip systems I which are activated as soon as the yield condition is violated

$$\Phi_I = \tau_I - \tau_y > 0 \rightsquigarrow \gamma_I = \gamma_0 \left[\left[\frac{\tau_I}{\tau_y} \right]^{1/m} - 1 \right] \tag{86}$$

Here γ_0 denotes the reference slip rate and m is the rate dependence parameter. To incorporate this type of rate dependence into the algorithm described above the viscoplastic evolution law for the slip rates γ_I is integrated by the Euler backward method and the result is subsequently reformulated into an implicit equation for the determination of the incremental slip rates $\Delta\gamma_I$

$${}^{n+1}\bar{\Phi}_I = {}^{n+1}\tau_I - \bar{\tau}_y \doteq 0 \quad \text{with} \quad \bar{\tau}_y = \tau_y({}^n\kappa + \Delta\kappa) \left[\frac{\Delta\gamma_I}{\Delta\gamma_0} + 1 \right]^m \tag{87}$$

Here, $\Delta\gamma_0$ abbreviates $\Delta t \gamma_0$. Note that this equation resembles the algorithmic consistency condition of the rate independent formulation and thus its implementation necessitates only marginal modifications to the basic algorithm. Moreover, it trivially reduces to the rate independent case by setting $m = 0$. Finally, one step of the local Newton iteration for the $\Delta\gamma_I$ is given in combination with a projection onto $\Delta\gamma_I \in \mathbb{R}_+$ in standard form as

$$\partial_{\Delta\gamma_I} {}^{n+1}\bar{\Phi}_I = -\eta_{IJ} - \bar{H}_{IJ} = -\bar{h}_{IJ}$$

$$\rightsquigarrow \Delta\gamma_I = \max\left\{ \left(\Delta\gamma_I + \sum_{J \in \mathcal{A}} \bar{h}^{IJ} \bar{\Phi}_J \right), 0 \right\}. \tag{88}$$

Thereby, the iteration operator $\bar{h}_{IJ}$ for the local Newton iteration is given with the algorithmic viscoplastic hardening moduli $\bar{H}_{IJ}$ which consist of two contributions resembling a kind of latent and self hardening

$$\bar{H}_{IJ} = H^{lat}(\Delta\gamma_I) + H^{slf}(\Delta\gamma_I)\delta_{IJ}$$

$$= H \left[\frac{\Delta\gamma_I}{\Delta\gamma_0} + 1 \right]^m + \frac{m\tau_y}{\Delta\gamma_0} \left[\frac{\Delta\gamma_I}{\Delta\gamma_0} + 1 \right]^{m-1} \delta_{IJ}. \tag{89}$$

Observe that the structure of the algorithmic tangent operator is preserved with only h^{IJ} substituted by $\bar{h}^{IJ}$. Thus, the singularity of the algorithmic tangent operator is excluded as long as

$$H^{lat} \neq 0 \quad \text{or} \quad H^{slf} \neq 0 \rightsquigarrow H \neq 0 \quad \text{or} \quad m \neq 0 \quad \text{and} \quad \tau_y \neq 0. \tag{90}$$

The resulting algorithm is formally identical to that summarized in Table 3 with only a few substitutions, e.g. for $\bar{\Phi}_I$, $\bar{\tau}_y$ and $\bar{H}_{IJ}$. It turns out in the computations that this formulation is much more robust even in the nearly rate independent limit which is obtained as $m \to 0$, e.g. by setting $m = 0.01$.

9
Compression problem of a square panel

This section is devoted to the analysis of a representative plane strain BVP incorporating single crystal plasticity. Thereby, it is our objective to compare the failure modes and load carrying capabilities for different orientations of the crystal slip systems with respect to the global laboratory frame.

The homogeneous square panel of single crystal material with side lenght of 10 mm is subjected to uniaxial compression between two rigid platens applied by displacement control, see Fig. 3. Thereby, the specimen is compressed quasi-statically with a constant process velocity of 10^{-3} mm/s until a maximum compaction of 4% is obtained. The contact between the platens and the specimen is modelled as ideal sticking thus enforcing an inhomogeneous displacement pattern. In order to capture localized failure modes and to avoid volumetric locking in quasi incompressible plain strain computations we employ **Q1E4** enhanced elements developed by (Simo and Rifai, 1990). The whole panel is discretized into 20 × 20 elements in order to allow for nonsymmetric failure modes which will automatically be triggered by nonsymmetric orientations of the slip systems with respect to the global axes.

The material parameters are chosen to model a nearly rate independent Al-Cu alloy with Lamé constants $L = 35104.88$ N/mm² and $G = 23427.25$ N/mm², initial shear yield stress $\tau_0 = 60.84$ N/mm², saturation strength $\tau_\infty = 109.51$ N/mm², initial hardening rate $H_0 = 541.48$ N/mm², rate sensitivity parameter $m = 0.01$ and reference shear strain rate $\dot{\gamma}_0 = 10^{-3}$. These material constants do not incorporate a softening behaviour into the constitutive description. Therefore, as a phenomenological model of damage effects, a linear softening term $H_s\kappa$ with $H_s = H_0/12$ is appended to the definition of the critical shear flow stress τ_y. For the kinematics of the crystal we assume the Asaro planar double slip model.

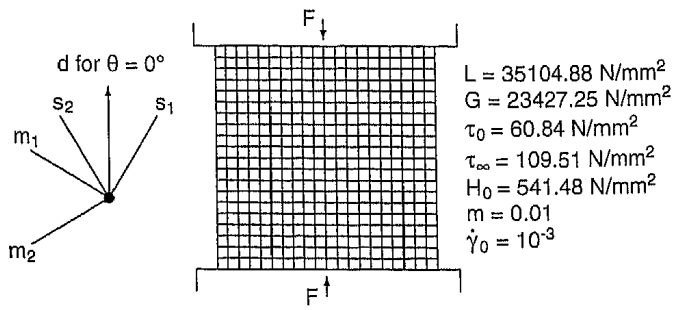

Fig. 3. Single Crystal Compression Problem of a Square Panel

Thereby the two slip planes are symmetrically oriented with $\pm 30^\circ$ about a $\boldsymbol{d}$ direction which itself is specified by the angle θ enclosed by the $\boldsymbol{d}$ the global $\boldsymbol{e}_2$ directions.

In the following we investigate slip system orientations which are characterized by $\theta = 0^\circ + n \times 15^\circ$ with $n = 0,1,2,3$. Thereby, different failure modes emerge. Moreover, it turns out that the computations for $n > 3$ render identical load carrying results compared to those obtained with $n \leqq 3$, whereby the deformed configurations are symmetric counterparts to those which are displayed in Figs. 4 to 7. Therefore, we exclusively concentrate on the cases with $n = 0,1,2,3$. In particular, the deformed configurations, magnified by five, in Figs. 4 and 5 for $n = 0$ and $n = 1$ document a strong tendency towards localized failure modes. On the other hand, Figs. 6 and 7 reveal a less emphasized shear band development. Obviously, the symmetric $\theta = 0^\circ$ slip system orientation results in a symmetric deformation mode. Counterintuitively, the non-symmetric $\theta = 45^\circ$ slip system orientation renders as well a symmetric deformation mode as displayed in Fig. 7. Remarkably, the shear band in Fig. 5 develops perpendicular to the orientation of the most active slip system 2.

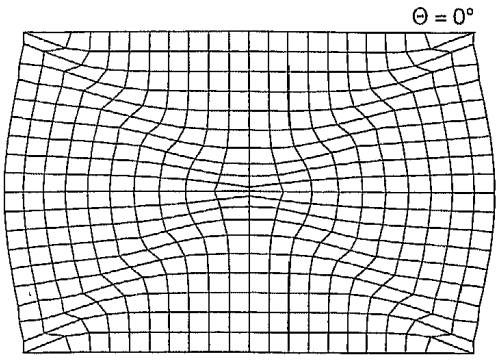

Fig. 4. Deformed Configuration $\theta = 0^\circ$

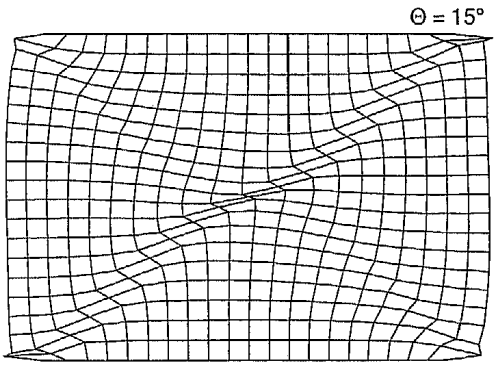

Fig. 5. Deformed Configuration $\theta = 15^\circ$

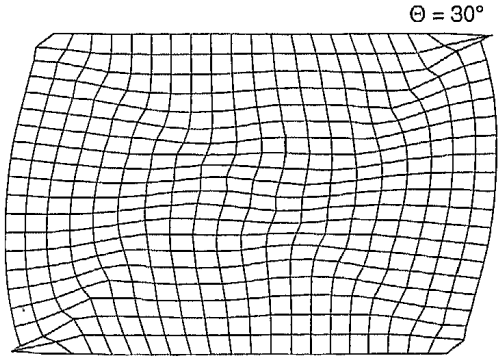

Fig. 6. Deformed Configuration $\theta = 30^\circ$

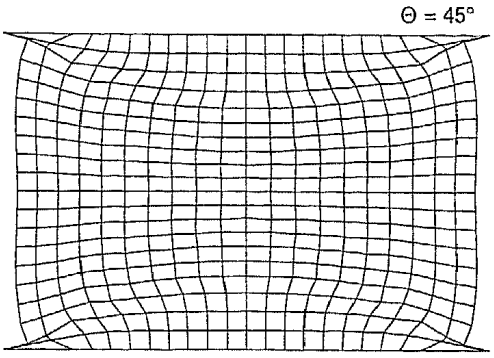

Fig. 7. Deformed Configuration $\theta = 45^\circ$

The resulting load displacement curves for the different orientations of the slip systems are reported in Fig. 8. Thereby, the peak load increases with the decreasing tendency towards localization. Moreover, it turns out that we obtain the identical results for the $n = 2$ and $n = 4$ as well as for the $n = 1$ and $n = 5$ orientation. Due to the small amount of softening introduced in order to model phenomenologically damage behaviour, the load deflection curves merely drop down very gently after peak load.

The tendency to develop localized or diffuse failure modes is reflected in the distribution of the internal variable κ depicted in Figs. 9 to 12. Again, in particular Figs. 9 and10 corresponding to the $\theta = 0^\circ$ and $\theta = 15^\circ$ slip system orientations clearly demonstrate localized failure modes. In contrast, the plastic zones in Figs. 11 and 12 are characterized by a rather diffused distribution.

Finally, the activity of the two slip systems is highlighted in Figs. 13 and 14 for the basic $\theta = 0^\circ$ case. Please note, that the incremental shear rates $\Delta\gamma_I$ associated with the individual slip

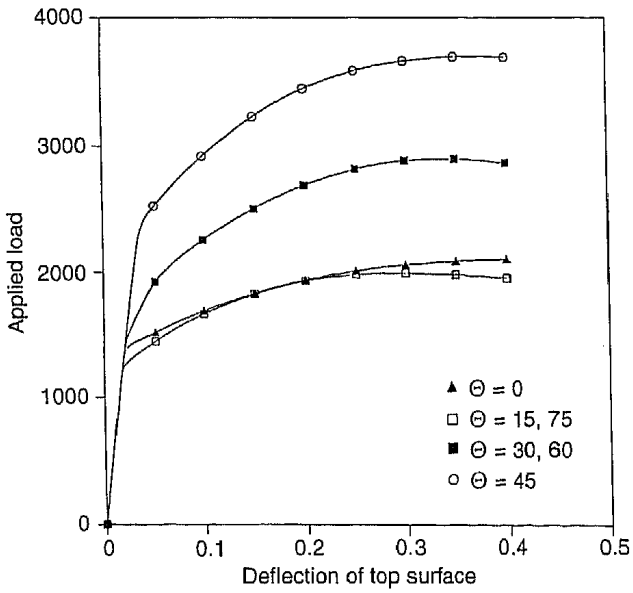

Fig. 8. Load Deflection Curves $\theta = 0^\circ$, $\theta = 15^\circ$, $\theta = 30^\circ$, $\theta = 45^\circ$

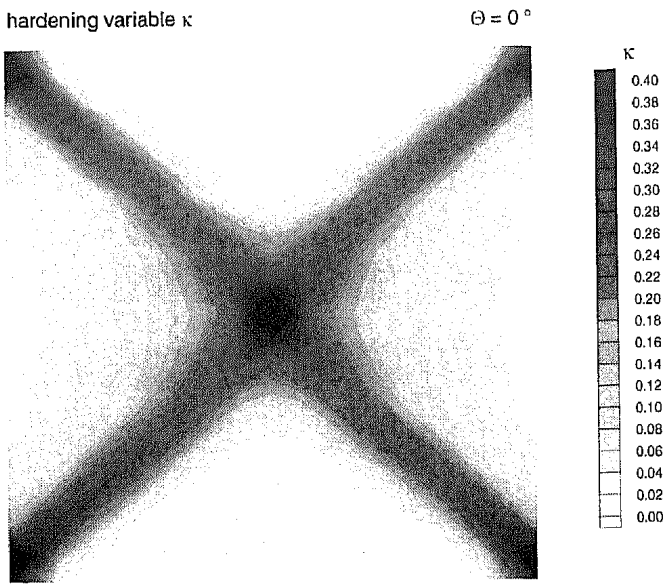

Fig. 9. Distribution of Hardening Variable $\theta = 0°$

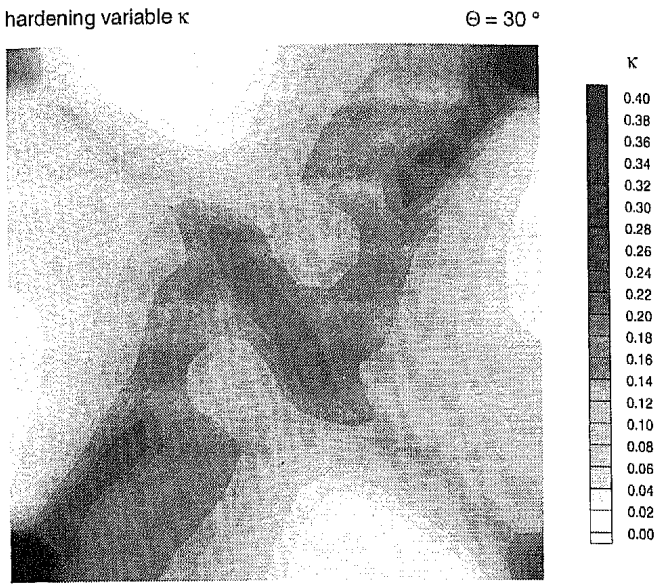

Fig. 11. Distribution of Hardening Variable $\theta = 30°$

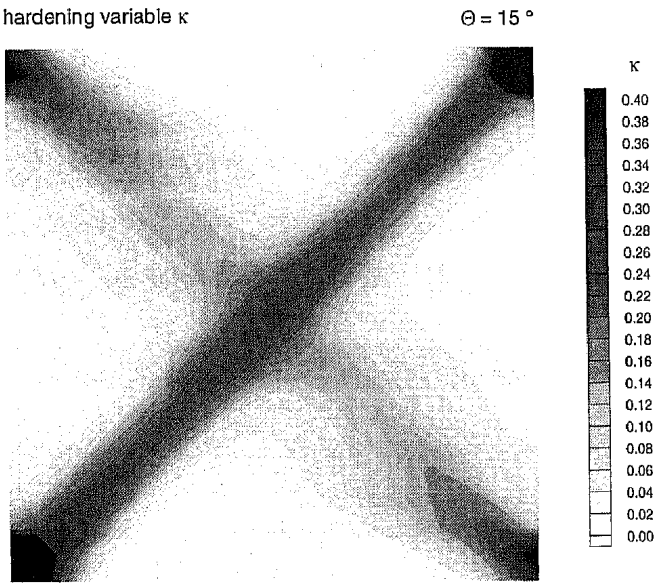

Fig. 10. Distribution of Hardening Variable $\theta = 15°$

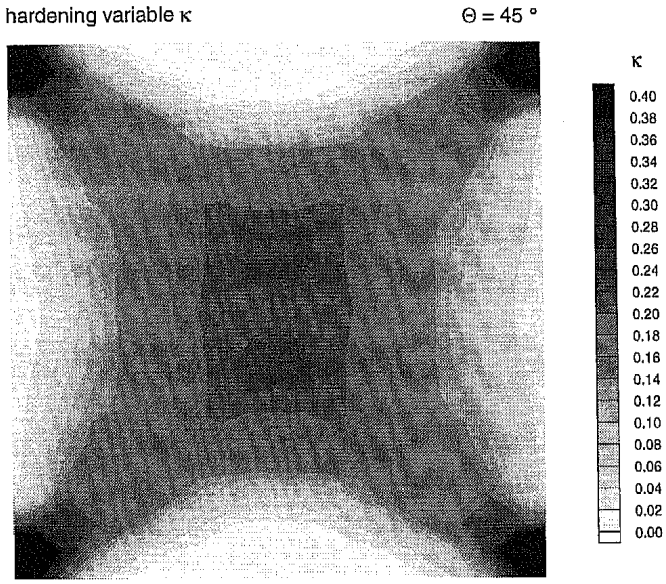

Fig. 12. Distribution of Hardening Variable $\theta = 45°$

systems take their maximum values within localized zones which are almost perpendicular to the orientation of the slip direction s_l.

10 Summary and conclusions

The objective of this work was the analysis of instability phenomena within the framework of multisurface elasto-plasticity.

To this end, first the condition for *diffuse* failure, characterized as the stationarity condition for the stress state, has been investigated. As a result, the elasto-plastic tangent operator loses positive definitness as soon as all active constraints cease to harden simultaneously with the space of critical strain rates spanned by the flow directions. Thereby, the analysis relied on the simple structure of the *multisurface* elasto-plastic tangent operator in the form of a sum of rank 1 updates which is subsequently mirrowed as well in the structure of the localization tensor.

The localization tensor has been the prime quantity in the subsequent establishment of the general localization or rather admissibility condition for the maintainance of a spatial discontinuity of the velocity gradient field. In this context we distinguished the conditions for the *onset* of *continuous* and *discontinuous* localization for the case of *multisurface* elasto-plasticity. Thereby, the basic case of *continuous* localization is characterized by further plastic loading of all active constraints on both sides of the anticipated discontinuity whereas in the limiting case of *discontinuous* localization the domain on the one side of the discontinuity completely unloads elastically while the domain on the other side continues loading plastically for all active constraints.

The investigation of the critical hardening moduli allowing for the *onset* of *continuous* localization in the general *multi-*

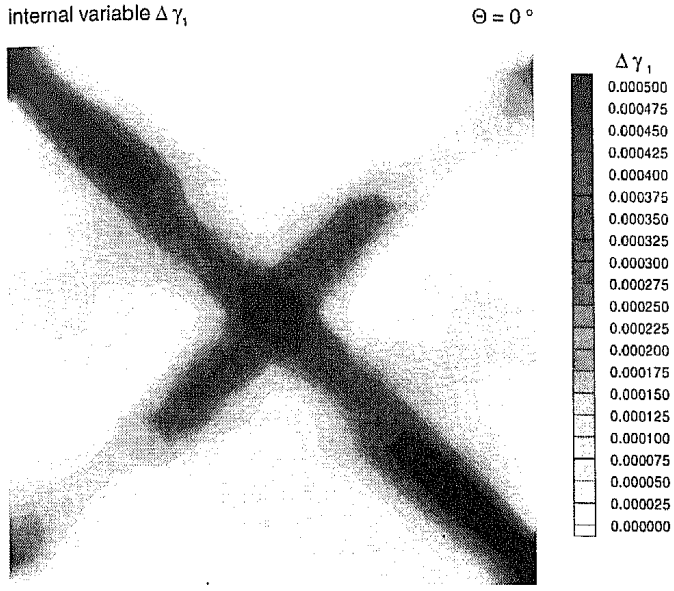

Fig. 13. Incremental Shear Rate 1. Slip System $\theta = 0°$

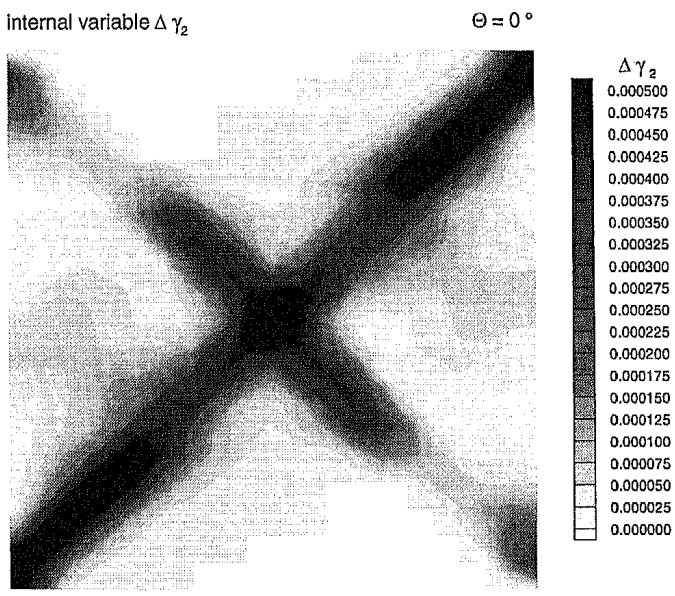

Fig. 14. Incremental Shear Rate 2. Slip System $\theta = 0°$

surface case then leads to a particular eigenvalue analysis to compute the determinant of a matrix with *multiple* rank one updates. As a result, for multiple active constraints the determinant of the localization tensor was conveniently evaluated in terms of the ω matrix containing the hardening moduli in a simple fashion. On the one hand, the critical hardening moduli, allowing for the onset of *continuous* localization, may be extracted from the ω matrix. On the other hand, the condition for the onset of *discontinuous* localization is determined by negative spectral properties of the symmetrized ω matrix. Thus, the analysis reveals the important result that in contrast to the *single surface* case *discontinuous* localization may precede *continuous* localization if *multiple* constraints are active.

The results for the general *multisurface* plasticity case with *multiple* active constraints were emphasized for the special cass of *triple*, *double* and *single surface* plasticity. As a major result, for a popular family of hardening laws the analysis of *continuous* localization boils down to the simple examination of the so-called $\bar{\eta}$ matrix to render the critical hardening moduli which allow for the onset of localization. Thereby, the remarkable simple results for either *latent* or pure *self hardening* of the slip systems, highlighting the characteristic similarities to the wellknown *single surface* case, have been elaborated.

As a numerical counterpart we briefly addressed the computational setting of *single crystal* plasticity as the paradigm for *multisurface* elasto-plasticity. The restriction to the geometrically linearized formulation allowed in particular for a simple and transparent integration algorithm. Thereby, to allow for rate dependent behaviour and to avoid the impending singularity of the tangent operator in the perfect plastic case, we applied a widely accepted extension of both the model and the algorithm by incorporating a viscoplastic evolution law for the slip rates. As a demonstration of the dramatic influence of the slip system orientation on the resulting localized failure mode and load carrying capacity of *single crystals* the algorithm has then been applied to the examination of a plane strain panel under compression.

In summary it is believed that the present work serves as an extension of the traditional localization analysis where only a single active constraint is taken into account by providing a canonical representation which allows for the examination of the localization properties in the general *multisurface* case.

References

Asaro, R. J. 1983: "Crystal Plasticity", J. Appl. Mech., ASME, Vol. 50, pp. 921–934

Boer, de R. 1982: Vektor- und Tensorrechnung für Ingenieure, Springer, Berlin etc.

Borja, R. I.; Wren, J. R. 1993: "Discrete Micromechanics of Elastoplastic Crystals", Int. J. Num. Meth. Engr., Vol. 36, pp. 3815–3840

Cuitiño, A.; Ortiz, M. 1992: "Computational Modelling of Single Crystals", Modelling Simul. Mater. Sci. Eng., Vol. 1, pp. 225–263

Hadamard, J. 1903: Leçons sur la propagation des ondes et les équation de l'hydrodynamique, Librairie Scientifique A. Hermann et Fils, Paris

Hill, R. 1958: "A General Theorie of Uniqueness and Stability in Elastic-Plastic Solids", J. Mech. Phys. Solids, Vol. 6, pp. 236–249

Hill, R. 1962: "Acceleration Waves in Solids", J. Mech. Phys. Solids, Vol. 10, pp. 1–16

Hill, R. 1966: Generalized Constitutive Relations for Incremental Deformation of Metal Crystals by Multislip", J. Mech. Phys. Solids, Vol. 14, pp. 95–102

Hill, R.; Havner, K. S. 1982: "Perspectives in the Mechanics of Elastoplastic Crystals", J. Mech. Phys. Solids, Vol. 30, pp. 5–22

Hutchinson, J. W. 1970: "Elastic-Plastic Behaviour of Polycrystalline Metals and Composites", Proc. R. Soc. London, A 318, pp. 247–272

Kocks, U. F. 1970: "The Relation between Polycrystal Deformation and Single-Crystal Deformation", Metall. Trans., Vo. 1, pp. 1121–1143

Koiter, W. T. 1960: "General Theorem of Elasto-Plastic Solids", in Progress in Solid Mechanics, Eds. I.N. Sneddon and R. Hill, North Holland Publishing Company

Mandel, J. 1962: "Ondes plastiques dans un milieu indéfini à trois dimensions", J. Mécanique, Vol. 1, pp. 3–30

Mandel, J. 1996: "Conditions de Stabilité et Postulat de Drucker", in Rheology and Soil Mechanics, Eds. J. Kravtchenko and P. M. Sirieys, Springer-Verlag, Berlin etc.

Mandel, J. 1972: "Plasticité Classique et Viscoplasticité", Cours au CISM No. 97, Udine '71, Springer, Berlin etc.

Miehe, C. 1994: "Multisurface thermoplasticity for Single Crystals at Large Strains in Terms of Eulerian Vector Updates", Int. J. Solids Struct., Vol. 33, pp. 3103–3130

Ottosen, N. S.; Runesson, K. 1991: "Properties of Discontinuous Bifurcation Solutions in Elasto-Plasticity", Int. J. Solids Structures, Vol. 27, pp. 401–421

Ramakrishnan, N.; Atluri, S. N. 1994: "On Shear Band Formation: I. Constitutive Relationship for a Dual Yield Model", Int. J. Plast., Vol. 10, pp. 499–520

Ramakrishnan, N.; Okada, H.; Atluri, S. N. 1994: "On Shear Band Formation: II. Simulation Using Finite Element Method", Int. J. Plast., Vol. 10, pp. 521–534

Rice, J. R. 1976: "The Localization of Plastic Deformation", in Theoretical and Applied Mechanics, Ed. W. T. Koiter, North Holland, Amsterdam etc.

Rizzi, E.; Maier, G.; Willam, K. 1996: "On Failure Indicators in Multi-Dissipative Materials", Int. J. Solids Struct., Vol. 33, pp. 3187–3214

Simo, J. C.; Kennedy, J. G.; Govindjee, S. 1988: "Non-Smooth Multi-surface Plasticity and Viscoplasticity. Loading/Unloading Conditions and Numerical Algorithms", Int. J. Num. Meth. Engr., Vol 26, pp. 1261–2185

Simo, J. C.; Rifai, M. S. 1990: "A Class of Mixed Assumed Strain Methods and the Method of Incompatible Modes", Int. J. Num. Meth. Engr., Vol. 29, pp. 1595–1638

Steinmann, P.; Stein, E. 1996: "On the Numerical Treatment and Analysis of Finite Deformation Ductile Single Crystal Plasticity", Comp. Meth. Appl. Mech. Engr., Vol. 128, 235–254

Watanabe, O.; Atluri, S. N. 1986: "Internal Time, General Internal Variable, and Multi-Yield-Surface Theories of Plasticity and Creep: A Unification of Concepts", Int. J. Plast., Vol. 2, pp. 37–57

Thomas, T. Y. 1961: Plastic Flow and Fracture of Solids, Academic Press, New York etc.